

## Quantum Swirling of Superfluid Helium Films

F. M. Ellis and L. Li\*

*Department of Physics, Wesleyan University, Middletown, Connecticut 06459*

(Received 23 June 1993)

Circularly polarized third-sound resonances are used to drive up and drive down persistent flow states in the superfluid  $^4\text{He}$  film inside the resonator, analogous to swirling a classical fluid by agitation. The induced flow states involve vortex densities pinned by the roughness of the substrate which can include left and right circulating vortices present simultaneously within the resonator. Densities are measured to be on the order of  $10^5/\text{cm}^2$ . The peak flow speed of the wave oscillations necessary to swirl the film are near the critical velocity for dc flow dissipation.

PACS numbers: 67.40.Vs, 67.40.Hf, 67.40.Pm, 67.70.+n

Third sound [1] is a wave mode which propagates in thin superfluid  $^4\text{He}$  films analogous to long wavelength gravity waves in water. The van der Waals attraction of the helium atoms to the substrate assumes the role of gravity and the macroscopic equations of motion are identical to the viscous-free hydrodynamics if aspects associated with the two fluid model [2] are ignored. There is an interesting qualitative distinction imposed by quantum mechanics: The circulation of vortices in the superfluid are quantized lending them a stability that their classical counterparts, subject to the inevitable diffusive effect of viscosity, do not have. We have used high amplitude third-sound resonances to change the vorticity present in the superfluid film, in effect, swirling the film in the resonator much like a fluid in a vessel swirled by subjecting the vessel to a circular shaking motion. Low amplitude resonances used as a probe of the resulting persistent flow fields have shown macroscopic deviation from curl-free potential flow, requiring large areal densities of vortices in the films at temperatures well below the superfluid transition. An equilibrium vortex density must be present in a rotating geometry [3]; however, the densities measured in this work are for a stationary substrate, and are in principle a nonequilibrium glass-like state. No evidence for relaxation of these densities has been observed.

There are two aspects related to the interaction of third-sound waves with the background flow which must be considered before interpreting the experiments: the Doppler shifting of the resonant modes as they propagate in the presence of a dc persistent flow field and the transfer of momentum and energy from the third-sound wave to that flow. The first of these has been previously used to detect circulation states inside of a third-sound resonator [4] and the second can be inferred from classical fluid mechanics and accepted dynamical properties of the quantized vortices [5]. The Doppler shifting of the modes will be summarized first.

Third-sound modes in a circular resonator are doubly degenerate in the absence of a background flow. If the basis states are taken as right and left polarized rotating waves, the asymmetry introduced by an annular flow field will shift the frequency of the mode traveling with the

flow up and the mode traveling against the flow down. The amount of the shift is determined by the details of the flow field and how it overlaps the mode's wave motion. The simplified equations of motion for the film can be taken as

$$\begin{aligned} \frac{dh}{dt} &= -\nabla \cdot (h\mathbf{v}), \\ \frac{d\mathbf{v}}{dt} + (\mathbf{v} \cdot \nabla)\mathbf{v} &= -\nabla(g h), \end{aligned} \quad (1)$$

for conservation of fluid and Euler's equation, respectively. The velocity terms will have two parts, one associated with the oscillatory wave fields and the other with the steady background flow. These expressions have been linearized in the wave fields and taken in the long-wavelength limit. The convective derivative must be retained because of the background flow. The boundary conditions assumed for solutions are that the radial velocity vanishes at the outer perimeter of the cell,  $r=a$ , and the height oscillations vanish at a small central hole at  $r=\epsilon a$ . The resonant frequencies of the solutions for a given flow field  $v_0(r)$  can be found either by perturbation (in  $v_0$ ) or by numerical integration. Expressing the results as

$$\frac{\Delta f}{f} = \gamma_m \frac{v_0(a)}{C_3}, \quad (2)$$

the unitless numbers  $\gamma_m$  give the shifts up and down of the modes in terms of the flow at the perimeter  $v_0(a)$  and the third-sound speed  $C_3 = \sqrt{gh}$ . It should be noted that the boundary condition at the hole has little effect on the results presented. These numbers depend on both the particular resonant mode, represented by  $m$ , and the functional form of  $v_0(r)$ . A measurement of this splitting for all of the modes could, in principal, be used to find  $v_0(r)$ , but with only a few modes experimentally convenient, only a "filtered" version of  $v_0(r)$  can be deduced, much like relying on a few terms of a power series to describe a function.

The inversion of the mode shifts used in the present analysis is based on an assumption of superposition. The validity of this assumption is supported by a general agreement of the splittings (2) calculated with the pertur-

bative approach [which has also been linearized in  $v_0(r)$ ] and the numerical integration. The flow field  $v_0(r)$  can then be deduced by the superposition of several model forms required to match the experimental splittings. Table I presents the values of  $\gamma_m$  used for three model flow fields with each of the three lowest resonant modes. The form proportional to  $1/r$  anticipates vorticity trapped in the hole, the form proportional to  $r$  allows for a uniform distribution of vorticity throughout the cell, and the constant flow form provides flexibility by adding an intermediate radial dependence to the vorticity distribution.

We now turn to the swirling interaction. The nonlinear and viscous terms omitted from the equations of motion (1) contain terms which for a traveling plane wave result in mean flow or streaming effects [6]. Mean flow refers to mass transport in high amplitude wave motion, and streaming is usually specifically associated with a time-averaged forward momentum transfer in the viscous boundary layer. Both of these effects are responsible for the swirling of fluid in a circular vessel by a circular agitation of the polarized wave states. In the case of a plane wave, one source of net forward momentum transfer can be envisioned as a consequence of an oscillatory drive force acting on a larger amount of material in the forward flow of the wave crests than in the reverse flow of the troughs.

How would the swirling in the superfluid case be achieved? In a resonator with the topology of a torus (as in the present case) and irrotational flow, a net circulation must be the result of a gain of quantized vorticity about the central hole. In terms of the film coating the torus, a vortex-antivortex pair must first be created somewhere in the film. The pair must then separate, with each half migrating in opposite directions around the circular cross section and their paths linking the hole, where they are reunited on the opposite side of the torus. Each such event would increase the classical fluid circulation by the quantized amount  $h/m_4$ . Many such events, say  $N_0$  of them, would swirl the film up to a large macroscopic flow state characterized by curl-free flow with  $v_0(r) = N_0 \hbar / m_4 r$ . If some of the vortices get stuck along the way, pinned to substrate features, the macroscopic flow field will deviate from a  $1/r$  form reflecting the net areal vortex density  $n(r)$  assumed to be axisymmetric:

$$v_0(r) = \frac{\hbar}{m_4 r} \left[ N_0 + \int_0^r n(r') 2\pi r' dr' \right]. \quad (3)$$

Creation of vortex pairs is expected for peak wave flows on the order of the Feynman critical velocity,  $\hbar/2m_4 d$ , with  $m_4$  the helium atom mass and  $d$  the film thickness. The migration mechanism of vortices in the presence of the wave motion must involve similar nonlinear effects as in the classical case but must also be combined with the problem of pinning and critical velocities in superfluids. In the case of bulk interaction with walls, this later problem is now fairly well understood [7]. We are unaware of any theoretical investigation of wave-induced mean flow

TABLE I. Doppler shift factors  $\gamma_m$  from Eq. (2) for the lowest three modes and flow fields used to model the persistent current circulation induced in the resonator.

Mode	Flow field $v_0(r)$		
	$v_0(a)(a/r)$	$v_0(a)$	$v_0(a)(r/a)$
$m=1$	1.24	0.159	0.089
$m=2$	1.17	0.630	0.409
$m=3$	1.13	0.755	0.549

in superfluid films, but the vortices are more likely to be depinned in the slightly larger backflow of the wave troughs. Here the Magnus force would deflect a right (left) circulating vortex to the left (right) of the wave propagation direction and as a result, increase the flow along the wave propagation direction. Although the origin of the mean flow is microscopic in the vortex description dictated by quantum mechanics, both the classical and quantum cases hinge on dissipative processes: classical viscosity in the first case and quantum vortex hopping or drag in the second.

The third sound is resonated in a superfluid film adsorbed on the inner surfaces of a flat, circular cavity formed between two gold-plated microscope slides. The perimeter is defined by epoxy which fills the gap for radii larger than  $a=6.15$  mm and holds the gap at  $8 \mu\text{m}$ . Electrically isolated regions of the gold coating serve as capacitive transducers which couple to the weakly dielectric helium film. Two drive regions at a  $90^\circ$  angular orientation allow circularly polarized drive forces to odd  $m$  modes. A single pickup region is incorporated as the capacitor of a 77 MHz  $L$ - $C$  tunnel diode oscillator so that the height oscillations in the film can be detected with standard frequency modulation techniques. A 0.13 mm radius central hole through both microscope slides provides film access to the interior of the resonator, and a toroidal topology favorable to circulation. The resonator and a  $10 \text{ m}^2$  surface reservoir are mounted together in a chamber on a dilution refrigerator.

The film is swirled by applying up to 30 V to the drive plates with a  $45^\circ$  phase shift. The drive forces are frequency doubled and the resulting  $90^\circ$  phase shift couples to the rotating traveling waves states. Once the mode is split by the circulation, the polarized drive is not necessary, although driving with only one of the drives is less effective. The mode is resonated at a high amplitude for a period of time, and the splittings are subsequently checked by observing the free decay of several modes at small amplitudes. The circulation strength is related to the frequency shifts of the split modes as described earlier, and the circulation direction can be determined for odd modes by interchanging the drives and observing the relative response to the left and right polarized drive. All circulations measured were absolutely stable in time at 0.12 K where all of the reported data were taken.

The circulation can be driven either up by driving the

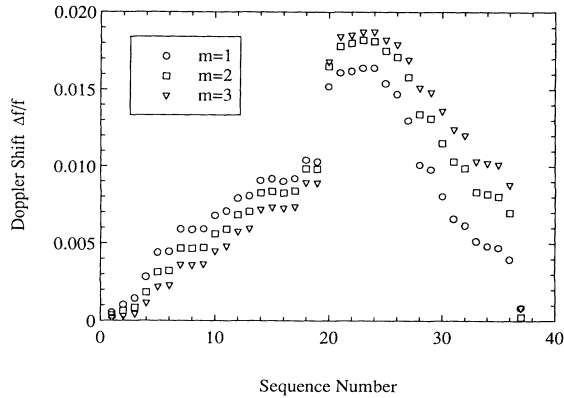


FIG. 1. Record of Doppler shifts as a fraction of the resonant frequency for the three lowest modes. The abscissa is for referencing the drive sequence procedure described in the text.

shifted up (+) mode or down by driving the shifted down (-) mode. Only the drive coupling to the  $m=1$  or  $m=2$  lowest modes was strong enough to change the circulation. Figure 1 shows the Doppler shifts  $\Delta f/f$  of the lowest  $m=1, 2,$  and  $3$  modes recorded over the course of about two weeks for a film in which the third-sound speed was  $17 \text{ m/s}$ . Starting with a film which has been warmed above the superfluid transition temperature to reset the circulation to near zero, the film was first driven up with the  $m=1^+$  (Fig. 1, 1-19) and  $m=2^+$  (20-24) modes, and then down with the  $m=1^-$  (25-34) and  $m=2^-$  (35-37) modes. Various drive voltages were used along the way, but the overall procedure swirled the film up as high as it would go with  $30 \text{ V}$ , and then back down. Two important features of this figure should be emphasized. First is that third sound is capable of changing the macroscopic quantum flow state of the superfluid film. A Doppler shift of roughly  $1.5\%$  (corresponding to the larger shifts of Fig. 1) along with the third-sound speed ( $1700 \text{ cm/s}$ ) indicates that persistent currents with speeds on the order of  $25 \text{ cm/s}$  have been induced by the third sound. This statement will be made more quantitative below but the second feature is even more interesting. Recalling that the form of the flow field is reflected in the relative shifts of the modes, it is clear from the reversal in magnitude of these shifts between readings around 15 and readings around 32 that the flow field must be deviating from a simple  $1/r$  form usually assumed for axisymmetric superfluid flow. This is direct evidence for stable pinned vortex densities in film since any flow form other than  $1/r$  requires such a density, shown by Eq. (3).

Figure 2 shows the results of measurements made at several points in the process just described that indicate at what third-sound amplitudes the swirling starts. The  $m=1$  resonance was swept through at  $0.0005 \text{ Hz/s}$  at increasing drive levels and the resulting third-sound height oscillations recorded. The resonant line shapes at the larger drives show deeply nonlinear behavior. From the maximum amplitude, the peak lateral flow speed of the

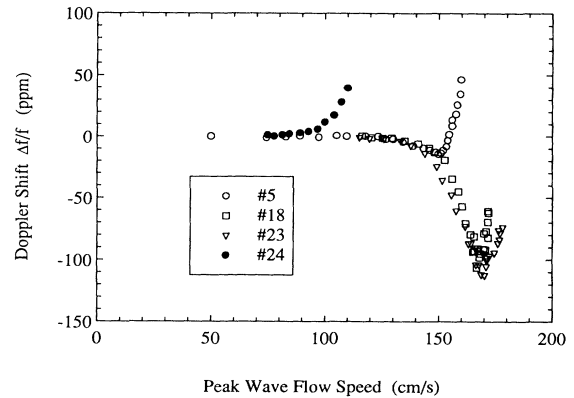


FIG. 2. Relative frequency change of the  $m=1$  mode for increasing third-sound peak lateral wave flow speeds. These curves represent the onset of swirling. All curves would continue to rise through the top of the graph if the data were continued to higher amplitudes. The numbers labeling the curves refer to position in Fig. 1.

wave motion was derived and taken as the abscissa in Fig. 2. The low amplitude free decay frequency of the same mode was carefully checked after each sweep for a change in the Doppler shift and plotted as the ordinate in ppm of the resonant frequency of  $810 \text{ Hz}$ . The data taking for each curve terminated when the frequency increased by more than  $10 \text{ ppm}$  or when  $30 \text{ V}$  was reached. The curves labeled 5, 18, and 23 (numbers refer to location in Fig. 1) were all taken driving the shifted-up mode ( $m=1^+$ ) to increase the circulation, although it should be noted that 23 was arrived at earlier by driving the  $m=2$  mode. Each initially loses circulation before finally rising as shown by the dip in the curves before the rise. This is further evidence for vortex pinning since not only are amplitudes above some threshold needed to swirl the flow up, but just below the threshold the wave motion tends to relax the persistent flow slightly by depinning some of the vortices. All curves would have continued to

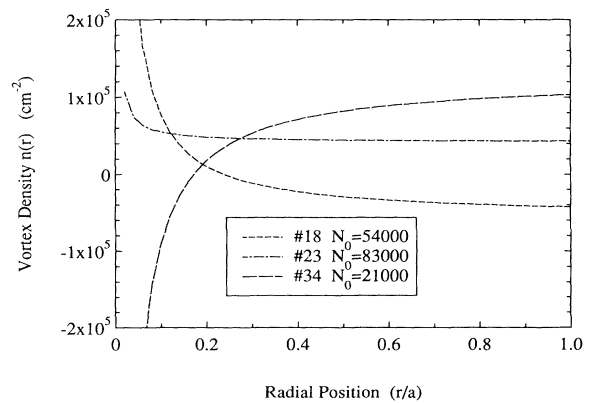


FIG. 3. Pinned vortex density deduced from the shifts of the lowest three modes at points referred to in Fig. 1. The total vorticity trapped in the central hole is included for each as  $N_0$ .

rise rapidly if the data were extended to higher drives. Curve 24 was taken subsequent to 23 but the shifted-down mode ( $m=1^-$ ) was driven to swirl the flow down. For this mode, the frequency shifts back up toward its unshifted value. There is evidently also a threshold for destroying the persistent current and it is noticeably lower. It should be noted that the Feynman critical velocity for this film is about 250 cm/s.

A description of both the flow fields and the pinned vortex density have been deduced from the relative mode shifts (2) and the relationship between the flow and the vortex density (3). Figure 3 shows the resulting vortex density distribution for conditions at position 18, 23, and 34. In each case the circulation quanta trapped in the central hole  $N_0$  (from the strength of the  $1/r$  terms in the model) are also shown to complete the description of where all of the vorticity is located. Keeping in mind that the modeling is based on only the lowest three modes, there is a clear indication of separation of positive and negative vortices consistent with the applied swirling sense. Driving with the  $m=1^+$  mode (18) creates vorticity of both senses near the center where the mode has its highest peak wave flow. One sense draws toward the center; the other sense gets pushed out toward the perimeter and possible annihilation with their counterparts from the opposite face. Driving the  $m=2^+$  mode (23) next, which has peak wave flows in the vicinity of  $r/a=0.6$ , continues the process of creation but is more efficient at moving the opposite sense vorticity out toward annihilation at the perimeter. Finally, driving the  $m=1^-$  mode (34) to swirl the flow opposite to its present direction reduces the vorticity trapped both in the hole and in the vicinity of the origin, with a resulting increase in the vorticity away from the center. Swirling in the opposite direction of the flow has clearly pushed vortices already present out toward the perimeter. Areal vortex densities on the order of  $50\,000/\text{cm}^2$  are involved, and the rotation sense of the vortices is not restricted to the same sense as the persistent current, which is positive throughout Fig. 1.

Are stable densities of pinned vortices of this size reasonable? The mean separation for a density of  $50\,000/\text{cm}^2$  is  $45\ \mu\text{m}$ , roughly 14 000 times the film thickness (3.2 nm). If the density of potential pinning sites is taken as the density of the "rolling hills" characteristic of scanning tunneling microscopy images of evaporated gold [8] then only  $10^{-6}$  of the hills need to pin a vortex. Numerical simulations of vortex pinning in bulk suggest that pinning sites will be even more prevalent since they can be of atomic dimensions [7]. The interaction between neighboring vortices at this density is negligible compared

to the integrated interaction among them all, the interaction responsible for the macroscopic flow field. This flow field, at an average speed of  $(\Delta f/f)C_3=25\ \text{cm/s}$ , is below that expected to cause depinning and therefore stability is not surprising. The maximum flows in all cases appear to be limited by near critical flow in the vicinity of the hole. This explains the large jump in Fig. 1 where driving with the  $m=2$  mode allowed a dramatic shift in the vortex density away from the center.

Third sound has been demonstrated to produce mean flows which remain as persistent currents in the macroscopic superfluid film state. The necessary third-sound amplitudes increase with the size of the flow already present, exhibiting a threshold near where the wave's peak lateral flow field approaches the critical velocities expected for dissipation of dc flow. This swirling of the film flow necessarily involves the creation and movement of vortices within the macroscopic quantum state of the superfluid. It is also evident from the form of the persistent current flow field that a substantial density of pinned vortices must be present in the film when it has been swirled. The stability of the experimental densities suggests that smaller densities of roughly equal numbers of both rotational senses could reasonably be an innate feature of any real superfluid film, perhaps a remnant of the Kosterlitz-Thouless transition [9] to the superfluid state.

We would like to thank Ralph Baierlein for insightful discussions and for his numerical investigations. We also thank the National Science Foundation and Wesleyan University for their support.

---

\*Present address: Department of Electrical Engineering, City College of the C.U.N.Y., New York, NY 10031.

- [1] D. Bergman, *Phy. Rev. A* **3**, 2058 (1971).
- [2] D. R. Tilley and J. Tilley, *Superfluidity and Superconductivity* (IOP, New York, 1990), Chap. 3.
- [3] P. W. Adams and W. I. Glaberson, *J. Low Temp. Phys.* **67**, 103 (1987).
- [4] F. M. Ellis and H. Luo, *Phys. Rev. B* **39**, 2703 (1989).
- [5] P. W. Adams and W. I. Glaberson, *Phys. Rev. B* **35**, 4633 (1987).
- [6] M. S. Longuet-Higgins, *Philos. Trans. R. Soc. London A* **245**, 535 (1953).
- [7] K. W. Schwarz, *Phys. Rev. Lett.* **69**, 3342 (1992).
- [8] B. L. Blackford, M. H. Jericho, and M. O. Watanabe, *Surf. Sci.* **276**, 122 (1989).
- [9] J. M. Kosterlitz and D. J. Thouless, *J. Phys C* **6**, 1181 (1973).